JET-COOLED SPECTROSCOPY OF THE *M*-XYLYL RADICAL IN A CORONA-EXCITED SUPERSONIC EXPANSION: HYPER-CONJUGATION AND CONFORMATIONAL DEPENDENCE IN VIBRONIC TRANSITIONS

Chang Soon Huh
Applied Chemistry Major, Division of
Chemical and Environmental
Engineering, College of Engineering
/Dong-eui University
South Korea

ABSTRACT

The electronically hot but jet-cooled *m*-xylyl radical was produced from the precursor *m*-xylene in a corona-excited supersonic expansion (CESE), and its vibronic emission spectrum was recorded. Theoretical studies of the ground and excited state structures, as well as the hyper-conjugative interaction of the *m*-xylyl radical, were carried out. The preferred geometry of the methyl rotor in the ground state is switched in the excited state. The vibronic emission spectrum of the *m*-xylyl radicals corresponded to the $D_1 \rightarrow D_0$ electronic transition and determined the electronic transition energy depending on the initial change in the methyl conformations.

Keywords: Spectroscopy, *m*-xylyl radical, corona discharge, hyper-conjugation, natural bond orbital.

1. INTRODUCTION

In combustion and atmospheric science, free radicals play an important role as reaction intermediates, while resonance-stabilized radicals have attracted significant attention due to their relatively high stability. The benzyl radical is a prototypical example of an aromatic hydrocarbon, and it has a rich history of experimental and theoretical studies [1-4]. Since the first observation of the benzyl radical [5], vibronic coupling and ring substitution have attracted much attention in the field of electronic spectroscopy. Vibronic coupling causes a significant change in the typical mirror symmetry between the ground and excited state spectra, while substitution on the benzyl radical perturbs the electronic structure and transition energy.

Methyl substitutions on the ring of benzyl are known to serve a variety of electronic structures, responding to changes in the orientation and the barrier height of the methyl group. In terms of methyl substitution, the xylyl radicals were studied by Schuler *et al*. [5] and Walker and Barrow [6] in the visible region. Bindley *et al*. assigned the xylyl radicals' strong bands from xylenes in a corona discharge [7]. Furthermore, the determination of the vibronic assignments and lifetime measurements of xylene was studied using the laser-induced florescence (LIF) technique by Charlton and Thrush [8].

Hiratsuka *et al*. [9] investigated the electronic energies of the close-lying doublet D_1 and D_2 states of the benzyl radical and described the possible vibronic coupling between the close-lying D_1 and D_2 electronic states. Cossart-Magos *et al*. [10] conducted a rotational contour analysis of the *o*-xylyl radical using the magnitude and direction of the transition dipole moment. Fukushima and Obi [4] utilized the high-resolution LIF technique to analyze the

vibronic coupling of the jet-cooled *p*-xylyl radical. Lin and Miller [11] determined the torsional bands of the methyl rotor in xylyl radicals, while Selco and Carrick [12] assigned the vibronic transition bands of benzyl and xylyl radicals.

Recently, Lee *et al.* [13-19] identified the fluorescence spectra of various benzyl-type radicals substituted with halogens (F, Cl) and methyl groups (dimethyl, tri-methyl) by applying corona-excited supersonic expansion (CESE). However, the methyl-substituted benzyl radicals have not been extensively analyzed due to the complicated vibronic structures and the torsional transitions in the CESE spectrum.

In this work, we describe the results of a spectroscopic analysis of the *m*-xylyl radical, which is generated from *m*-xylene in the corona discharge. The emission spectrum of the *m*-xylyl radical contains two kinds of electronic state that are related to the methyl conformations in the ground and excited states. For the analysis of the observed spectrum, the spectroscopic data concerning the electronic transition and vibrational mode frequencies are analyzed with the help of the *ab initio* calculation. In addition, the energy change in the methyl conformation of the ground state is discussed using a natural bond orbital (NBO) analysis to explain the hyper-conjugation and energy differences in the methyl group's orientation.

2. EXPERMENTAL AND THEORETICAL METHODS

The experimental condition of this work was accomplished using the apparatus described by Han, Choi, and Lee [20]. Briefly put, we used conditions that play an important role in the favorable generation of substituted benzyl radicals in a corona excitation.

Reagent grade *m*-xylene (the precursor) was purchased from Sigma-Aldrich and then used without further purification. The concentration of the precursor was believed to be less than 1% of the He carrier gas at an ambient temperature. The gas mixture was expanded through a 0.2–0.3 mm in diameter glass nozzle connected to a vacuum chamber pumped using an 800 L/min mechanical rotary pump [21]. A high voltage (5 mA at 2000 V) was applied to a stainless steel rod that ran the length of the glass tube to within almost 0.5 mm of the opening. After a corona discharge was induced at the nozzle's opening, a blue-green colored jet could be seen in the benzyl-type radicals in the $D_1 \rightarrow D_0$ transition. The 5 mm light jet area of the nozzle opening was collimated and focused on the slit of a 2 m monochromator containing two 1800 lines/mm gratings. It was detected using a cooled Hamamatsu R649 photomultiplier tube and a photon counting system. During the scans, the monochromator slits were typically set to 100–200 μm, providing a resolution of about 2 cm^{-1}. A spectrum ranging from 19,800 to 22,000 cm^{-1} was acquired in 2.0 cm^{-1} increments over 2 hours. The Helium (He) atomic lines observed in the same spectral region as the benzyl-type radicals were used as calibration points [22].

Theoretical calculations were performed to study the D_0 and D_1 states using the density functional theory (DFT) method. The geometries of the ground states were optimized at the hybrid density functional B3LYP level using a 6-311+G (d, p) basis set [23, 24]. The vibrational frequencies of the benzyl-type radicals were computed in order to analyze the vibronic structures with a scaling factor of 0.987. Time-dependent (TD) formalism was employed to obtain the vertical excitation energies and excited state geometries of the benzyl-type radicals with a 6-311+G** basis set [25-30]. A population analysis was also performed using the natural bond orbital method at the B3LYP/6-311+g (d, p) level of theory using the NBO method [31] with a GAUSSIAN 09 program [32].

3. RESULTS

3. 1 CESE spectrum

A vibronic emission spectrum using *m*-xylene as the radical precursor is shown in Figure 1.

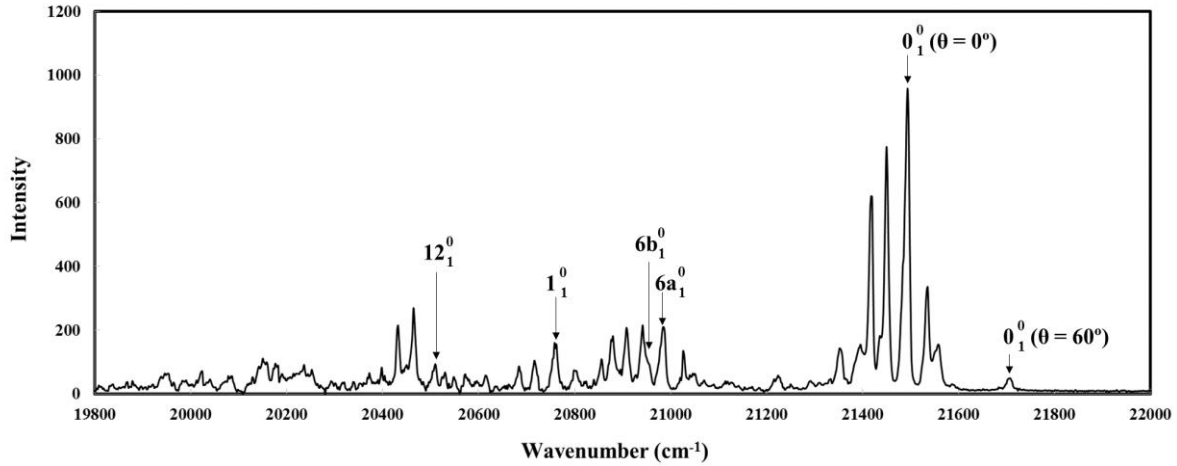

Figure 1. A portion of the fluorescence emission spectrum of the *m*-xylyl radical produced from *m*-xylene in a corona discharge. Several vibronic bands are labeled.

This spectrum includes a number of sharp lines between 19,800 and 22,000 cm^{-1}. The electronic origin is assigned to the intensive peak at 21,494 cm^{-1}, which is in good agreement with the previously reported values of 21,486 and 21,473 cm^{-1} for the *m*-xylyl radical [11, 12]. No hot bands are observed, which suggests that the molecules were cooled efficiently in the CESE. According to Lin and Miller, the cluster peaks of each vibronic band are caused by internal methyl rotation [11]. The vibronic peak assignments are discussed later in this paper. The emission spectra of the benzyl and methyl-substituted benzyl radicals using CESE shows sharp lines, which is in agreement with previously reported spectra [12-21]. The benzyl radical has an origin band with a weak intensity at 22,002 cm^{-1}. As the benzyl radical is substituted into the benzene ring, the origin band shifts to a lower wavenumber. The origin bands of the *o*- and *p*-xylyl [3] radicals are observed at 21,345 and 21,704 cm^{-1}, respectively, indicating that they have shifted 657 and 298 cm^{-1} from the benzyl radical, respectively. The 2, 6-dimethylbenzyl [5] and 3, 5-dimethylbenzyl [7] radicals have origin bands at 20,616 and 20,842 cm^{-1}, respectively. In a previous study, Selco and Carrick reported *o*- and *p*-xylyl radicals from an *m*-xylene precursor, and they explained the isomeric products to result in benzyl valence- or primase-type intermediates that correspond to photolysis and pyrolysis. However, in the present study, bands were identified for the *o*-xylyl radical, but not for the *p*-

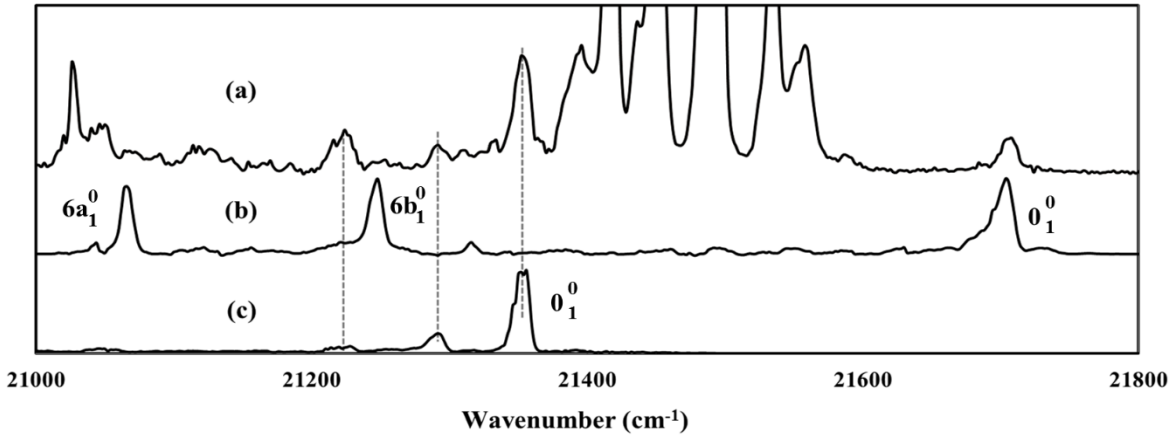

xylyl radical.

Figure 2. A portion of the visible emission spectra in the $D_1 \rightarrow D_0$ transition observed in the CESE of (a) *m*-xylyl, (b) *p*-xylyl, and (c) *o*-xylyl radicals.

Figure 2 shows a spectra comparison of the *m*-xylyl radical from *m*-xylene with the *o*- and *p*-xylyl radicals. In the comparison, the torsional and vibronic bands of the *o*-xylyl radical are included in the *m*-xylyl radical, while the 21,706 cm^{-1} peak has shifted 2 cm^{-1} from the origin of the *p*-xylyl radical and the *p*-xylyl's intensive vibronic bands (6a and 1 modes) are not observed. This means that the 21,706 cm^{-1} band is not the origin of the *p*-xylyl radical and hence it is likely to be the transition band from species in the excited state of the *m*-xylyl radical.

3. 2 Theoretical results

Theoretical calculations were performed to confirm the structure and spectral assignments. Figure 3 displays the calculated structural parameters, and the D_0 state optimized geometries show differences from the D_1 state. The values in parentheses indicate the ring angle (˚). The optimized geometries for the *m*-xylyl radical in the ground and first excited states show dominant changes in the bond length in the aromatic ring. The bond lengths in the aromatic ring increase, while the benzylic C-C bond length decreases in the first excited state. The internal rotation of the methyl group in the *m*-xylyl radical was investigated in both the D_0 and D_1 states.

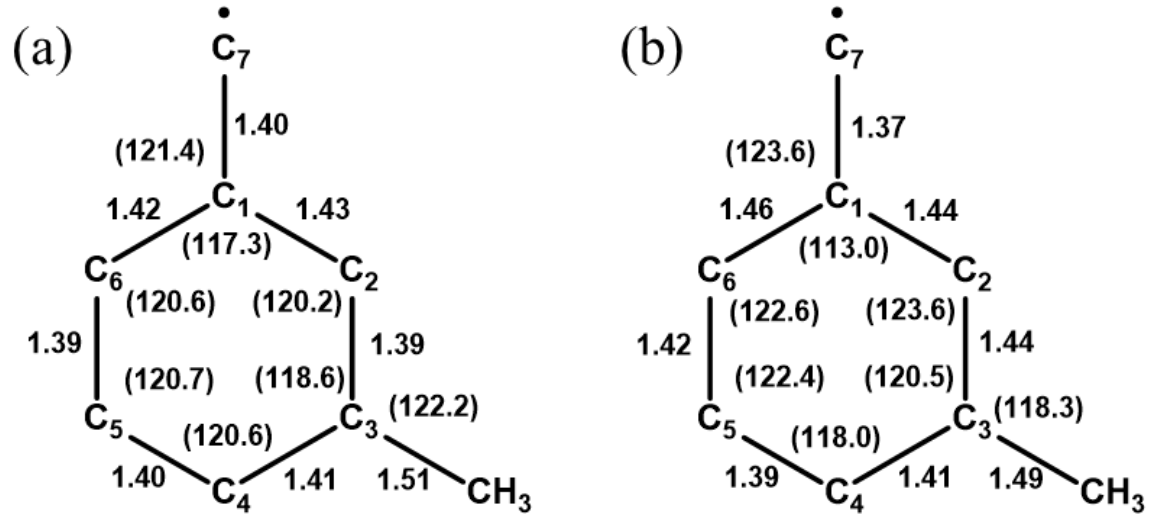

Figure 3. Geometries of the *m*-xylyl radicals in (a) the ground (D_0) state and (b) the first excited state (D_1) optimized at the B3LYP/6-311+G (d, p) level of theory. The bond length in Å and the bond angles in degrees are given in parentheses.

Figure 4 exhibits the potential energy curves of the *m*-xylyl radical in the D_0 and D_1 states as a function of the rotational angle (θ) of the methyl group. The rotational barrier of the *m*-xylyl radical in the D_0 state is calculated to be a small barrier that becomes larger upon $D_0 \rightarrow D_1$ excitation, which shifts the rotational phase of the methyl groups.

Molecule	B3LYP/6-311+g(d, p)	Experimental torsional barrier (cm^{-1})

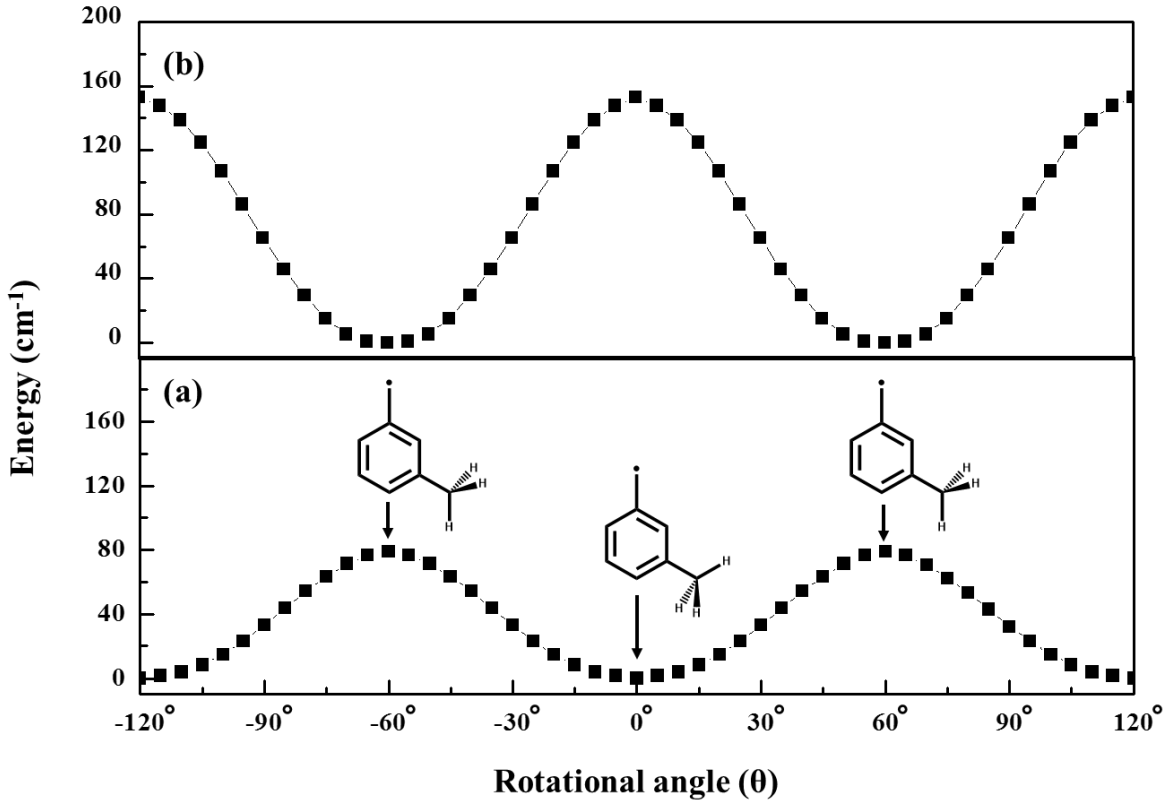

Figure 4. Potential energy curves of the methyl rotation (θ) in (a) the ground state (D_0) and (b) the first excited state (D_1).

Table 1 lists the methyl torsional energy of the xylyl radicals and toluene derivatives in the ground state. The meta-substituted toluene derivatives and *p*-xylyl have a small energy barrier between 1 ~ 25 cm^{-1}. However, the *m*-xylyl radical has a relatively higher barrier at 79 cm^{-1} with a different stable methyl conformation (θ = 60˚). In order to explain the mechanism of the conformation and the rotational barrier of the *m*-xylyl radical, we performed steric and NBO analyses. Figure 3 shows the geometrical parameters in the D_0 state and D_1 state, which were optimized using the TD-DFT calculation. The maximum changes in the bond lengths and bond angles are 0.04 Å and 4.4°, respectively, while the average values are 0.03 Å and 2.0°, respectively.

Molecule	Torsional barrier (cm^{-1})	Stable conformation (θ) *Ab initio* B3LYP/6-311+g(d,p)	Experimental Torsional barrier (cm^{-1})
m-xylyl	79	0	74[a]
p-xylyl	2.6	30	4[a]
m-xylene	21.3	30	25[b]
p-xylene	22.4	30	10[b]
m-fluorotoluene	16.2	60	16.9[c]
p-fluorotoluene	2.8	30	4.8[c]
m-chlorotoluene	1.6	60	8[d]
p-chlorotoluene	6.8	30	17[d]

Structure

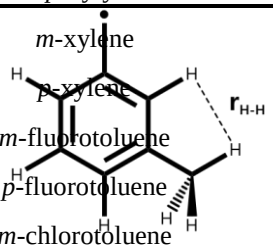

(θ = 0)

D_0 (Å)	D_1 (Å)
2.374	**2.332**

Table 1. Torsional potential barrier in the ground state for the xylyl radicals and toluene derivatives.

[a] Reference [11].
[b] Reference [33].
[c] Reference [34].
[d] Reference [35].

As shown in Table 2, the distance between the hydrogen of the methyl group and the adjacent hydrogen of the benzene ring provides steric information, and the differences in distance are 0.01 Å and 0.08 Å in the D_0 and D_1 states, respectively. Although we can identify a change in the structure of the *m*-xylyl radical, the changes are quite small in the D_0 state due to the relatively high internal rotation barriers.

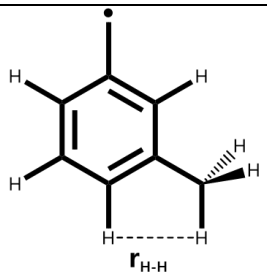 **(θ = 60˚)**	**2.382**	**2.413**
Δ **$[r_{H-H}(\theta = 0^{\circ}) - r_{H-H}(\theta = 60^{\circ})]$**	**0.008**	**0.081**

Table 2. Calculated H-H distance between the methyl group and benzene ring in the D_0 and D_1 states for the different conformation angles (θ).

To investigate the ground state conformation, we conducted an NBO analysis of the D_0 state. An NBO analysis is a useful technique for analyzing intra- and intermolecular bonding and interaction in the molecular bonds, as well as providing a proper basis for researching conjugative interactions in filled and virtual orbital spaces [36]. Some electron donor orbital, acceptor orbital, and interacting stabilization energy resulting from the second-order micro-disturbance theory have been reported [37, 38]. The larger the E (2) value, the more intensive the interaction between the electron donors and the greater the extent of the conjugation of the whole system. The delocalization of electron density between occupied Lewis-type (bond or lone pair) NBO orbitals and formally unoccupied (antibonding or Rydberg) non-Lewis NBO orbitals corresponds to a stabilizing donor-acceptor interaction. Furthermore, the NBO analysis was performed on the *m*-xylyl radical at the B3LYP/6-311+G (d, p) level in order to elucidate the high energy barrier and conformation change in the ground state. The molecular interaction is formed by the orbital overlap between the σ(C-C) and σ*(C-C) bond orbitals, which results in an intramolecular charge transfer (ICT) that causes a stabilization of the system. These interactions are observed as an increase in the electron density in the C-C antibonding orbital that weakens the respective bonds.

Electron	Donor(i)	Type	Acceptor	Type	$E^{(2)}$ (θ = 0˚) (kcal/mol)	$E^{(2)}$ (θ = 60˚) (kcal/mol)
Alpha	C1-C2	π	C3-C4	π^*	19.7	18.9
Alpha	C3-C4	π	C5-C6	π^*	16.0	15.3
Alpha	C5-C6	π	C1-C2	π^*	12.1	11.9
Alpha	C7	LP	C1-C2	π^*	34.7	34.4
Beta	C1-C2	π	C7	LP^*	37.3	37.1
Beta	C1-C2	π	C5-C6	π^*	11.8	11.7
Beta	C3-C4	π	C1-C2	π^*	18.1	17.4
Beta	C5-C6	π	C3-C4	π^*	14.5	13.8
Beta	C7	LP	C1-C2	π^*	19.5	18.0
Beta	C1-C2	π^*	C3-C4	π^*	132.4	145.6
Beta	C1-C2	π^*	C5-C6	π^*	102.8	0.0

Table 3. Second-order perturbation energy values between the occupied and anti-

bonding orbitals of the *m*-xylyl radical (θ = 0˚ and 60˚) using an NBO basis.

Table 3 shows the most important interactions between the Lewis and non-Lewis orbitals, the second-order perturbation energy values, E (2), corresponding to the conformation of θ = 0° and 60° of the methyl rotor angle. A strong interaction was observed between the p-type orbital containing the lone electron of C7 and the π*(C1–C2), π*(C3–C4), π*(C5–C6), and LP*(C7) anti-bonding orbitals of the benzyl structure in the alpha and beta spins. One of the strongest interactions (102.8 kJ mol^{-1}) between the π*(C1–C2) and π*(C5–C6) is calculated on an angle θ = 0° of the methyl rotor in the beta spin. However, this intensive stabilization energy is not computed at θ = 60° of the methyl rotor. The strong intra-molecular hyper-conjugation interaction between the π* → π* electrons in the ring leads to the stabilization of the (θ = 0°) *m*-xylyl radical. This interaction confirms the conformational difference of the *m*-xylyl radical in the D_0 state, which is distinguishable from the *p*-xylyl radical and other methyl-substituted toluene as shown in Table 2.

The theory also suggests that two *m*-xylyl radical conformations (θ = 0˚ and 60˚) could be observed in the discharge as displayed in Figure 5. The TD-DFT calculation predicts the $D_1 \rightarrow D_0$ transition energy for *m*-xylyl (θ = 0˚) to be 232 cm^{-1} higher than the $D_1 \rightarrow D_0$ transition energy calculated for the *m*-xylyl (θ = 60˚) conformation.

3. 3 Vibronic transitions

The emission spectrum for the $D_1 \rightarrow D_0$ transition in the *m*-xylyl radical is expected to exhibit an intense origin band with a few vibronic transitions corresponding to aromatic ring vibrations, since the optimized geometries for the ground and first excited state of the *m*-xylyl radical are nearly identical. The intense origin band in Figure 1 is consistent with the findings of previous studies [11, 12]. Different minimum conformations of the methyl rotor in the ground and first excited states suggest that the emission spectra for each species should be different and distinguishable.

Figure 5 indicates a possible collision relaxation process of the *m*-xylyl radical and emissions caused by conformational differences in the ground and excited states. Since there were a number of collisions inside the nozzle prior to expansion, the collisional relaxation of the excited states is an important factor in CESE. By means of collisional relaxation, the vibronic transition from *m*-xylyl (θ = 60°) should be stronger than the transition from *m*-xylyl (θ = 0°) that is a condition of the collision process in the excited states. The strongest energy

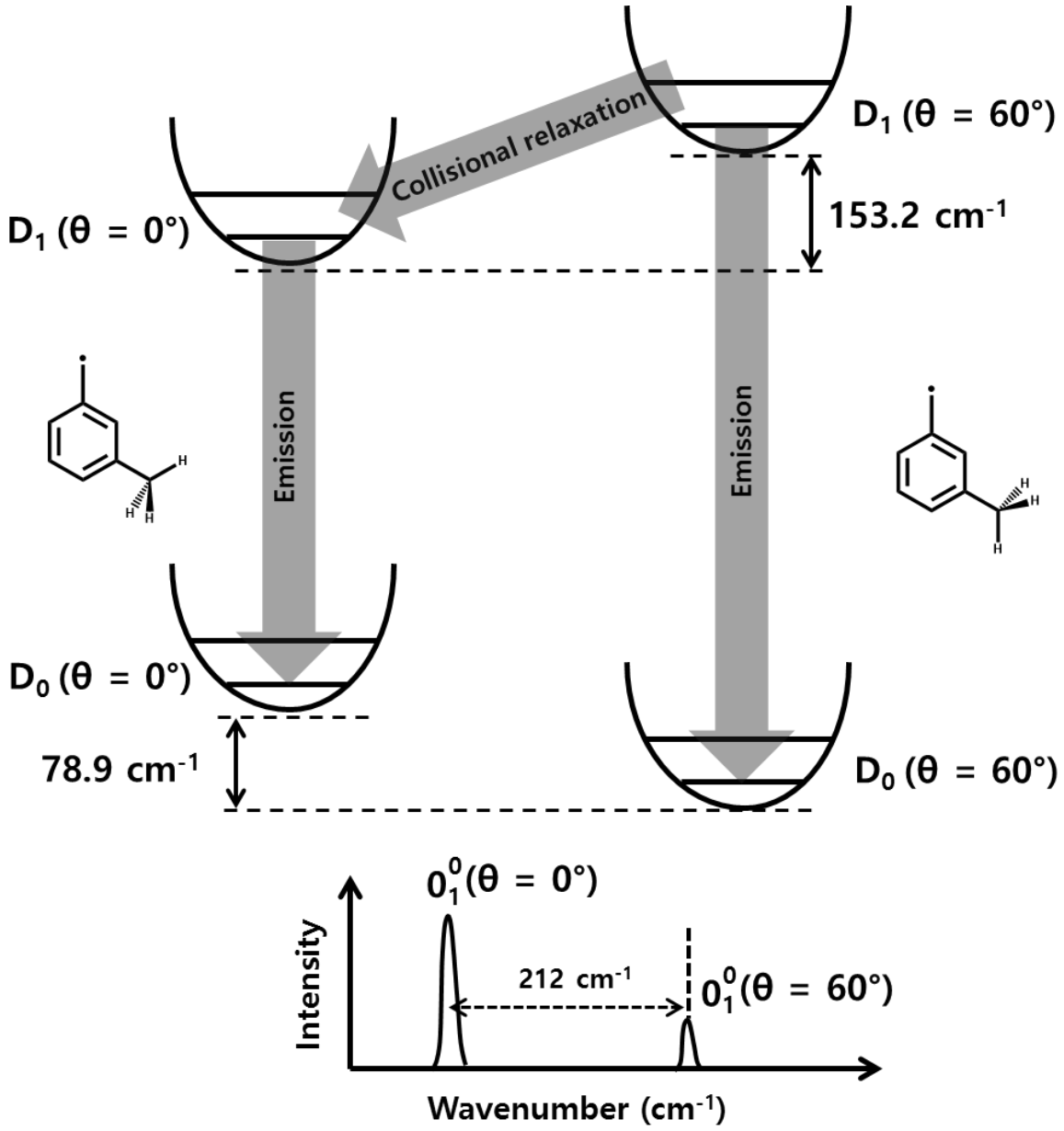

peak of 21,494 cm^{-1} is assigned as the origin of the *m*-xylyl (θ = 0°), while the 21,706 cm^{-1} band is assigned as the origin of the *m*-xylyl (θ = 60°). The experimental energy difference of 212 cm^{-1} between the two conformations (θ = 0° and 60°) is accordant with the calculated energy difference of 232 cm^{-1}. Although we assigned the origin of the *m*-xylyl (θ = 60°), vibronic bands of conformation (θ = 60°) were not observed due to a weak transition intensity and overlapping among the strong bands of the *m*-xylyl (θ = 0°).

Figure 5. Possible emission processes of the *m*-xylyl radical at the CESE and the assignment of the transition origin from the different methyl conformations.

Internal methyl torsional transitions are observed as cluster peaks around the origin band

and several vibronic bands. Table 4 lists the experimental bands observed in this work together with their assignments. The peaks were assigned with the assistance of the *m*-xylene precursor vibrations and the calculated frequencies for the ground state of the *m*-xylyl radical as listed in Table 5.

Position	Intensity	Spacing[b]	Assignment
21706	w	-212	Origin (θ=60˚)
21590	vw	-96	4e-1e
21558	s	-64	$3a_1$-$0a_1$, $3a_2$-$0a_1$
21536	vs	-42	2e-1e
21494	vs	0	Origin (θ=0˚)
21450	vs	44	1e-2e
21418	w	76	$0a_1$-$3a_2$, $0a_1$-$3a_1$
21396	w	98	1e-4e
21354	w	142	1e-5e, *o*-xylyl origin
21292	w	198	$0a_1$-$6a_1$, *o*-xylyl 2e-2e
21224	w	266	1e-7e, *o*-xylyl 4e-4e
21046	w	448	$6a^0_1$ + $3a_1$-$0a_1$, $3a_2$-$0a_1$
21026	m	468	$6a^0_1$ + 2e-1e
20984	m	510	$6a^0_1$
20954	w	540	$6b^0_1$
20942	m	552	$6a^0_1$ + 1e-2e
20908	m	586	$6a^0_1$ + $0a_1$-$3a_2$, $0a_1$-$3a_1$, $6b^0_1$ + 1e-2e
20878	m	616	$6b^0_1$ + 1e-2e
20856	w	638	$6b^0_1$ + 1e-4e, *o*-xylyl $6b^0_1$
20802	w	692	1^0_1 + 2e-1e
20760	m	734	1^0_1
20716	w	778	1^0_1 + 1e-2e
20684	w	810	1^0_1 + $0a_1$-$3a_2$, $0a_1$-$3a_1$
20616	vw	878	*o*-xylyl 1^0_1
20572	vw	922	$7b^0_1$
20510	vw	984	12^0_1
20464	m	1030	12^0_1 + 1e-2e
20432	m	1062	12^0_1 + $0a_1$-$3a_1$, $0a_1$-$3a_1$
20372	vw	1122	12^0_1 + 1e-5e
20236	w	1258	13^0_1
20190	vw	1304	13^0_1 + 1e-2e
20180	w	1314	14^0_1
20158	w	1336	13^0_1 + $0a_1$-$3a_1$, $0a_1$-$3a_1$, 3^0_1

Mode[a]	*This work*[b] (D_0)	*Ab initio*[c] B3LYP/6-311+g(d,p) (D_0)	*Precursor*[d] (S_0)
Mode[a]	*m*-xylyl radical		*m*-xylene
Origin	0		
6a	510	510	515
6b	540	541	535
1	734	734	723
7b	922	920	903
12	984	978	1003
13	1258	1268	1252
14	1314	1308	1264
3	1336	1325	1303

Table 4. List of the observed vibronic bands and their assignments. [a]
[a] Measured in a vacuum (cm^{-1}).
[b] Spacing from the (θ = 0˚) origin band at 21,494 cm^{-1}.

Table 5. Vibrational frequencies (cm^{-1}) of the *m*-xylyl radical.
[a] Reference [39].
[b] Measured in a vacuum (cm^{-1}).
[c] Multiplied by a scaling factor of 0.987.
[d] Reference [40].

4. DISCUSSION

The three major peaks are assigned as the 6a, 6b, and 1 vibrations, which are commonly observed in the spectra of benzyl-type radicals. These assignments demonstrate a good level of agreement with similar assignments in previous studies of mono-, di- and tri-methyl benzyl radicals [13-16]. The strong vibronic bands at 20,984 cm^{-1} shift by 510 cm^{-1} from the origin band, and the $6a_1^0$ band of the *m*-xylyl radical is a very important vibrational mode of C-C-C angle deformation, which is degenerated in benzene at about 606 cm^{-1}. The splitting between 6a and 6b increases with the substituents' increasing mass. By means of the splitting at 30 cm^{-1} for *m*-xylyl, the 6b mode is overlapped with the 6a torsional bands. To distinguish the 6b mode and its torsional bands, the vibronic bands are convoluted and assigned to the 6b vibration at 20,954 cm^{-1} as shown in Figure 6.

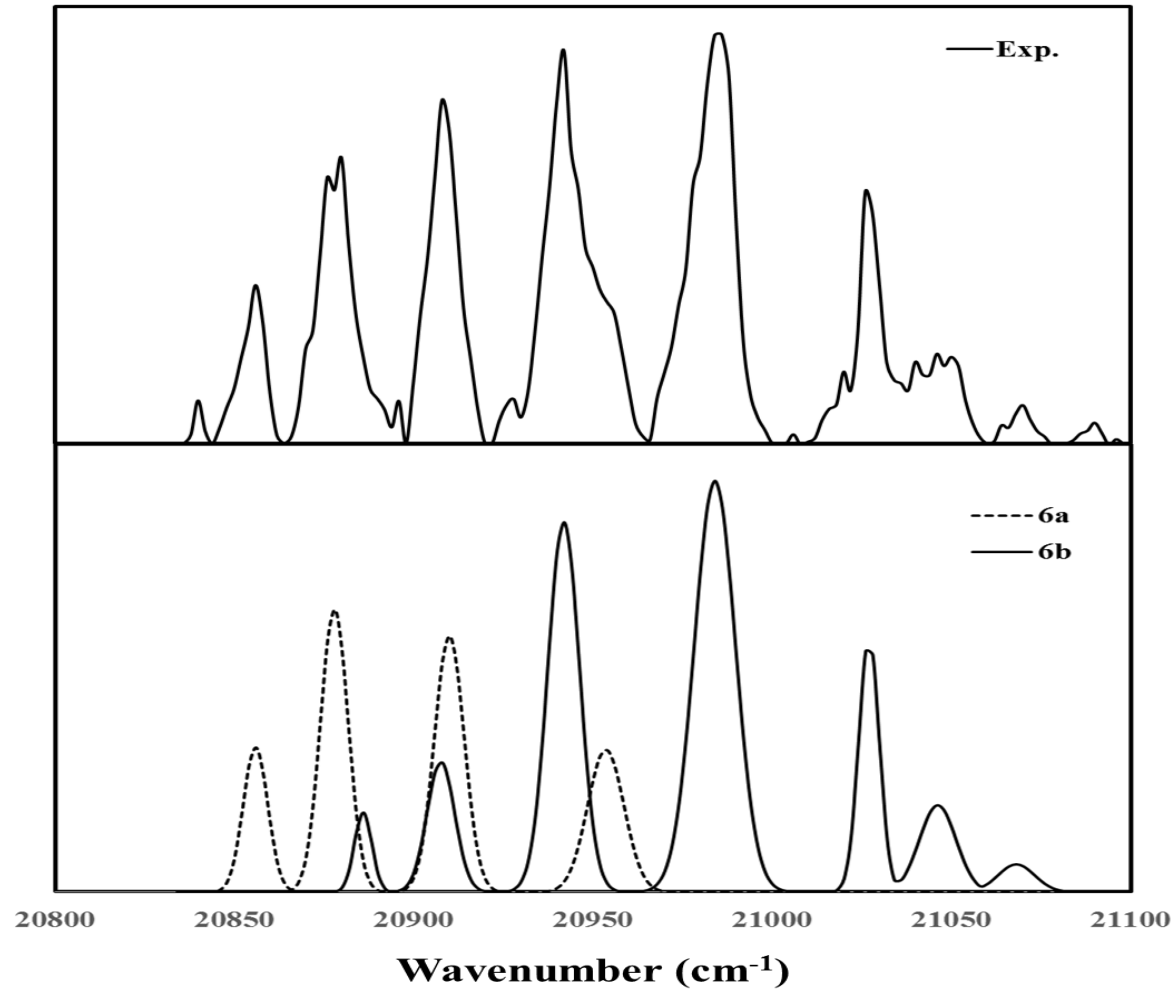

Figure 6. Peak-fitting result of the CESE bands constituted with 6a and 6b.

The peak-fitting bands are based on the parameter of origin and 12 vibronic bands with the Gaussian function. The band at 20,760 cm^{-1} was assigned to the 1_1^0 of the ring breathing vibration, which is consistent with that of the precursor, *m*-xylene. The weak peak at 20,572 cm^{-1} corresponds with the $7b_1^0$. The two peaks at 20,510 cm^{-1} and 20,236 cm^{-1} are assigned to the 12_1^0 and 13_1^0 bands, respectively. All the assigned vibronic bands (6b, 6a, 1, 12, 7b, 12, and 13) relate to the ring vibration mode that belongs to in-plane vibration.

From the calculations for the *m*-xylyl radical, a total of 45 vibration mode frequencies was obtained, of which 30 and 15 modes belong to in-plain (a') and out-of-plane (a'') vibration, respectively. The calculated values have been multiplied by a scaling factor of 0.987 in order to correlate with the observed values, as in the case of the *m*-xylyl radical. In Table 5, the observed and calculated vibrational mode frequencies of the *m*-xylyl radical are listed with those of *m*-xylene.

5. CONCLUSIONS

This study reports the gas-phase emission spectrum of the *m*-xylyl radical. Two possible $D_1 \rightarrow D_0$ transitions could be formed by conformational changes in the ground and excited states from the *m*-xylene precursor. Theoretical studies of the conformation changes reveal that the ground state has strong stabilization due to the hyper-conjugative interaction, which results in a small conformational barrier in the ground state. From the analysis of the spectrum, we assigned the observed spectra of the

θ = 0° and θ = 60° conformational *m*-xylyl radical to the $D_1 \rightarrow D_0$ electronic transition. The experimental origin reported in this study is in good agreement with the previously reported values related to corona discharge and LIF on the *m*-xylyl radical. The assignment was supported by previous methyl-substituted benzyl radicals, vibrational mode analysis, and *ab initio* calculations. The experimental vibrational energies were in good agreement with the theoretical predictions.

ACKNOWLEDGEMENTS

This work was supported by a research grant from Dong-Eui University.

REFERENCES

[1] C. Cossart-Magos, S.J. Leach. (1976) Chem. Phys. 64, 4006.
[2] G.C. Eiden, J.C. Weisshaar. (1996) J. Chem. Phys. 104, 8896.
[3] J.I. Selco, P.G. Carrick. (1989) J. Mol. Spectroscopy. 137, 13.
[4] M. Fukushima, K. Obi. (1990) J. Chem. Phys. 93, 8488.
[5] H. Schuler, L. Reinbeck, A.R.Z. Kaberle. (1952) Naturforsh. 7A, 421.
[6] S. Walker, R.F. Barrow. (1954) Trans. Faraday Soc. 50, 541.
[7] T.F. Bindley, A.T. Watts, S. Watts. (1962) Trans. Faraday Soc. 58, 849.
[8] T.R. Charlton, B.A. Thrush. (1986) Chem. Phys. Lett. 125, 547.
[9] H. Hiratsuka, K. Mori, H. Shizuke, M. Fukushima, K. Obi. (1989) Chem. Phys. Lett. 157, 35.
[10] C. Cossart-Magos, D. Cossart, S. Leach. (1974) Chem. Phys. 1, 306.
[11] T.-Y.D. Lin, T.A. Miller. (1990) J. Chem. Phys. 94, 3554.
[12] J.I. Selco, P.G. Carrick. (1995) J. Mol. Spectroscopy. 173, 277.
[13] G.W. Lee, S.K. Lee. (2006) J. Chem. Phys. A 110, 1812.
[14] G.W. Lee, S.K. Lee. (2006) J. Chem. Phys. A 110, 2130.
[15] G.W. Lee, S.K. Lee. (2007) J. Chem. Phys. 126, 214308.
[16] G.W. Lee, S.K. Lee. (2007) J. Chem. Phys. A 111, 6003.
[17] Y.W. Yoon, C.S. Huh, S.K. Lee. (2012) Chem. Phys. Lett. 550, 58.
[18] Y.W. Yoon, C.S. Huh, S.K. Lee. (2012) Chem. Phys. Lett. 525, 44.
[19] C.S. Huh, Y.W. Yoon, S.K. Lee. (2012) J. Chem. Phys. 136, 174306.
[20] M.S. Han, I.S. Choi, S.K. Lee. (1996) Bull. Korean Chem. Soc. 17, 991.
[21] S.K. Lee. (2002) Chem. Phys. Lett. 358, 110.
[22] M.L. Weise, M.W. Smith, B.M. Glennon. (1966)Atomic Transition Probabilities, NSRD-NBS4, Gaithersburg, MD.
[23] C.T. Lee, W.T. Yang, R.G. Parr. (1988) Phys. Rev. B 37, 785.
[24] A.D. Becke. (1993) J. Chem. Phys. 98, 5648.
[25] G. Scalmani, M.J. Frisch, B. Mennucci, J. Tomsi, R. Cammi, V. Barone. (2006) J. Chem. Phys. 124, 094107.
[26] F. Furche, R. Ahlrichs. (2002) J. Chem. Phys. 117, 7433.
[27] M.E. Casida, C. Jamorski, K.C. Casida, D.R. Salahub. (1998) J. Chem. Phys. 108, 4439.
[28] R.E. Stratmann, G.E. Scuseria, M.J. Frisch. (1998) J. Chem. Phys. 109, 8218.
[29] R. Bauernschmitt, R. Ahlrichs. (1996) Chem. Phys. Lett. 256, 454.
[30] C. Van Cailie, R.D. Amos. (2000) Chem. Phys. Lett. 317, 159.
[31] E.D. Glendening, A.E. Reed, J.E. Carpenter, F. Weinhold. (1998) J. Am. Chem. Soc. 120, 12051.
[32] M.J. Frisch et al. (2009) Gaussian 09, Gaussian, Inc.: Wallingford, CT.
[33] P.J. Breen, J.A. Warren, E.R. Bernstein, J.I. Seeman. (1987) J. Chem. Phys. 87, 1917.
[34] K. Okuyama, N. Mikami, M. Ito. (1985) J. Phys. Chem. 89, 5617.

[35] H. Kojima, K. Sakeda, T. Suzuki, T. Ichimura. (1998) J. Phys. Chem. A 102, 8727.
[36] M. Sarafran, A. Komasa, E.B. Adamska. (2007) J. Mol. Struct (Theochem.) 827, 101.
[37] C. James, A. Amal Raj, R. Reghunathan, I. Hubert Joe, V.S. Jayakumar. (2007) J. Raman Spectrosc. 37, 1381.
[38] L.J. Na, C.Z. Rang, Y.S. Fang, J. Zhejiang. (2005) Univ. Sci. 6B, 584.
[39] E.B. Wilson. (1934) Phys. Rev 45, 706.
[40] G. Varsanyi. (1974) Assignments for Vibrational Spectra of Seven Hundred Benzene Derivatives, John Wiley & Sons, New York, NY.